ATCA detects cometary-shaped objects in the giant H II region NGC 3603

A. Mücke[1]

Université de Montréal, Département de Physique

CP 6128, Succ. centre-ville, Montréal

P. Québec, H3C 3J7, Canada

B.S. Koribalski

Australia Telescope National Facility, CSIRO

P.O. Box 76, Epping 1710, Australia

A.F.J. Moffat[1]

M.F. Corcoran

Goddard Space Flight Center, NASA/GSFC Code 661

Laboratory for High Energy Astrophysics, 20771 Greenbelt, MD, USA

I.R. Stevens

School of Physics & Astronomy, University of Birmingham

Birmingham B15 2TT, UK

Received _____; accepted _____

ALTERNATIVE TITLES, PLEASE CHOOSE ONE ONLY, OR A COMBINATION (OF SEVERAL) WHICH MAKE SENSE ;-)

-Radio imaging of proplyd-like nebulae in NGC 3603

-Massive proplyd-like nebulae in NGC 3603: the radio image

-Radio detections of cometary-shaped objects in the giant H II region NGC 3603

-Non-thermal radio emission from proplyd-like clumps in NGC 3603

-ATCA (or Radio) imaging of the proplyd-like objects in NGC 3603

nterstellar medium: H II regions: individual (NGC 3603) — stars: pre-main-sequence — stars: early type, interferometry — stars: formation

1. Introduction

The giant H II region NGC 3603, located at a distance about 6 kpc, shows the densest concentration and largest collection of visible massive stars known in our Galaxy. Recent HST images of $\sim$0.″2 angular resolution (Moffat et al. 1994) have shown that NGC 3603 consists of 3 Wolf-Rayet (WR) stars and $\sim$70 O-type stars, with an estimated 40–50 being located in the central crowded region with about 30″×30″of size. The 3 H-rich WR-stars of subtype WNL are also located in the core and are the brightest members of the cluster. They are believed to be massive main sequence stars which, like the bright stars in R136a, drive very strong winds (De Koter et al. 1997; Crowther and Dessart 1998).

Ultracompact (UC) H II regions are small (<0.1 pc) nebulae, *internally* photoionized by a deeply embedded, massive star. Even though the stars are very luminous, they are invisible at optical wavelengths because of the surrounding dust; instead they show strong far-infrared emission. Their radio continuum emission is often associated with OH and H_2O masers. The morphology of UC H II regions in high resolution radio continuum images

ranges from spherical, cometary, core-halo, shell, to irregular (Wood and Churchwell 1989).

In contrast, a proto-planetary disk (ProPlyD) is a phenomenon describing a low-mass, young stellar object (YSO) with a circumstellar disk, embedded in a dense (neutral and ionized) envelope that is being *externally* photo-evaporated by the ultraviolet radiation from one or more massive stars. These low-mass stars are not able to ionize their surrounding significantly. The disks in these systems are either observed directly (e.g. most disks of the Orion ProPlyDs are seen directly or in silhouette against the bright background nebula (Bally et al. 2000)), or are inferred because in almost all of the ProPlyDs (young) low-mass stars are visible at optical or near-infrared wavelengths (see e.g. Stecklum et al. (1998)). At low angular resolution ProPlyDs look like UC H II regions, but at very high resolution optical and near-infrared images reveal their different nature. So most ProPlyDs would have been classified as UC H II regions prior to those observations. In some cases the distinction between the two classes remains difficult. Given the fact that there are about four times more UC H II regions than expected (REF??) from star formation rates and the potential problems identifying host stars for UC H II regions (e.g. some may not have enough FIR flux to account for an internal OB star), it may well be that a large fraction of catalogued UC H II regions are mis-identified ProPlyDs.

Interferometric radio continuum observations of ProPlyDs are needed to determine their structure, spectral indices and thus the nature of their emission, as well as mass loss rates and extinctions when compared to measured Hα fluxes.

The first identification of ProPlyDs was made in the Orion Nebula (O'Dell et al. 1993). Two more ProPlyDs have been identified in more distant nebulae; one in NGC 2024 by Stapelfeldt et al. (1997) and one, G5.97-1.17, in the Lagoon Nebula by Stecklum et al. (1998). The three ProPlyDs in NGC 3603 (Brandner et al. 2000) are the biggest, youngest

and most massive ones found *so far*. They are also the most distant known. [2]

Brandner et al. (2000) report the discovery of three ProPlyD-like structures in NGC 3603. These emission nebulae are clearly resolved in the HST/WFPC2 observations, and share the overall morphology of the ProPlyDs in Orion. All three nebulae are rim-brightened and tear-drop shaped with the tails pointing away from the central ionizing cluster.

According to Brandner et al. (2000) the brightest nebula (ProPlyD 1), which has a projected distance of 1.3 pc from the cluster, has the spectral (excitation) characteristics of a UC H II region. The optical spectra reveal the presence of an underlying, heavily reddened continuum source, which is also confirmed by near-infrared VLT/ISSAC observations. The WFPC2 observations show that only the outermost layer is ionized whereas the interior is neutral. The morphology of ProPlyD 1 is described as a heart-shaped head with a collimated structure in between, which can be understood as the superposition of actually two individual ProPlyDs. In contrast, ProPlyD 2 and 3, located at a distance of 2.2 pc and 2.0 pc from the stellar cluster, respectively, show approximately axisymmetric morphology. No embedded disk or central star could be detected so far in these nebulae, rendering a clear identification as proto-planetary disks. The optical point source (see Fig. 2c) close to ProPlyD 3 is probably not physically linked to the ProPlyD (Brandner et al. 2000).

---

[2]There is a variety of different 'words' used in the literature for describing the knots of ionised gas in M 42 (Orion); e.g. CKs (cometary knots), PIGs (partially ionized globules), EIDERS (external ionised (accretion) disks in the environs of radiation sources), and ProPlyDs (proto-planetary disks); for a summary see McCullough et al. (1995). Another 'word' being used is EGGs (for evaporating gaseous globules) describing the objects found in M 16 (Eagle Nebula). The cometary knots found in the Helix Nebula are compact globules and very different from ProPlyDs as they contain no stars.

The ProPlyD-like structures in NGC 3603 are about two orders of magnitude fainter than typical UC H II regions, but have a typical extent of 9000 AU with tails extending to 21000 AU, much larger in size than the ProPlyDs in Orion (see Table 4).

Recent 3.4 cm radio continuum and recombination lines measurements of NGC 3603 by De Pree et al. (1999), which were focussed on abundance measurements and the bright continuum emission from the ionized gas in this region, have an angular resolution of only $\sim 7''$ and very poor sensitivity (5σ = 55 mJy). By obtaining high sensitivity and high angular resolution ($\sim 1''$–$2''$) *ATCA* observations we primarily aimed to study the winds from many of the early-type stars mostly in the cluster core, as well as to detect and resolve the ProPlyDs and other gaseous regions in the cluster periphery. This paper will focus on the ProPlyDs[3] only, which have been detected and are shown to be clearly resolved. A subsequent paper containing a detailed study of the whole NGC 3603 region based on our *ATCA* observations will follow.

2. Observations and Data Reduction

Radio continuum observations of NGC 3603 were made with the Australia Telecope Compact Array (*ATCA*) in the 6A, B and D configurations in three observing runs in February, April, and June 2000 with a total of 36 hours assigned observing time. The observing frequencies were 4.8 GHz (6 cm) and 8.64 GHz (3 cm) with a bandwidth of 128 MHz each. Detailed observing parameters are given in Table 1. The three data sets were combined, reduced and analysed in MIRIAD using standard procedures. The full Stokes

[3]Throughout this paper we use the term "ProPlyD" for these cometary-shaped objects in NGC 3603 though we wish to note, that the identification of these objects as ProPlyDs is not clear yet, owing to the so far non-detection of a central disk or star.

parameters were measured. The flux density scale was calibrated using observations of the primary calibrator, 1934–638, assuming flux densities of 2.84 and 5.83 Jy at 3 and 6 cm, respectively.

A primary beam correction was carried out. To obtain high angular resolution and filter the extended emission to emphasize the small scale structure we used uniform weighting of the *uv* data while omitting the shortest baselines $< 25\,\mathrm{k}\lambda$, respectively. After this procedure the average r.m.s. in the combined radio maps is about 0.08 mJy at 3 cm and 0.41 mJy at 6 cm, but varies throughout the map. The r.m.s. level near the ProPlyDs, which are lying in rather empty regions, is ~ 0.1 mJy at 3 cm and ~ 0.2 mJy at 6 cm. This is close to the theoretical r.m.s. of about 0.053 mJy at 3 cm and 0.056 mJy at 6 cm. The dynamic range in the 3 and 6 cm images is about 1:100. Fitting a 2D-Gaussian to the dirty beam gives FWHM values of $0\farcs95 \times 0\farcs77$ at 3 cm and $1\farcs61 \times 1\farcs27$ at 6 cm. Since we are aiming to fit the observed ProPlyD-like structures to circular Gaussians, we have restored the cleaned maps with a circular Gaussian beam of width $0\farcs95$ at 3 cm and $1\farcs61$ at 6 cm, thus resulting in a slight decrease of the resolution in the present radio maps.

To create the spectral index maps between 3 and 6 cm we convolved the 3 cm map with a Gaussian appropriate to achieve a resolution of $1\farcs61$, the beam FWHM at 6 cm. The spectral index maps were then derived from the 6 cm and convolved 3 cm map using a clip value of 0.8 mJy beam^{-1}, corresponding to approximately 8σ at 3 cm and 4σ at 6 cm. Error maps for the spectral index maps were calculated using error propagation.

EDITOR: PLACE TABLE 1 HERE.

3. Results

Three proto-planetary disks in the giant H II region NGC 3603, originally found by HST+VLT (Brandner et al. 2000), have been detected with the ATCA at 3 and 6 cm (see Fig. 1). All three ProPlyDs are clearly resolved, showing a head-tail extent of $\sim 4''$ (see Fig. 2). Proplyd 3 shows the most pronounced head-tail structure with a 3 cm flux density ratio between head and tail of about 10 : 1. The tail is very well defined and at least $2''$ long, pointing away from the central star cluster. Unfortunately, ProPlyD 3 is rather faint in the low-sensitivity HST broad band image shown by Brandner et al. (2000); it is located outside the region of their high-sensitivity HST Hα image.

3.1. ProPlyD structure and fluxes

The three ProPlyDs have a cometary or head-tail shape[4] at cm-radio wavelengths, matching their appearance in optical images (see Fig. 2). To describe their radio structure in more detail we have fitted circular Gaussians[5] to the brightest component of each ProPlyD and studied the residual maps (i.e. the resulting maps after subtracting the fitted Gaussians; see Fig. 3). The latter show the uncertainty of the Gaussian fit as well as any remaining structures, i.e. the ProPlyD tails. Our best-fit parameters of the Gaussians, which are interpreted as the ProPlyD heads, as well as the residual fluxes in the region of the ProPlyD tails are summarized in Table 2. The residual $\sigma_{\rm fit}$ at the location of the head is used to estimate flux uncertainty in the Gaussian fitting: $\sigma^2 = \sigma^2_{\rm fit} + \sigma^2_{\rm rms}$, where $\sigma_{\rm rms}$ is

[4]The silhouette of ProPlyDs has variously been referred to as cometary, tadpole, tear-drop or simply head-tail shaped.

[5]We find that elliptical Gaussians instead of circular ones would fit too much tail flux to the head.

the r.m.s. in the map.

The radio heads of the ProPlyDs are typically 2″–3″ in diameter (see Table 2) while the total head-tail extent is ∼4″. ProPlyD 3 shows the most pronounced head-tail structure of the three (most likely due to the viewing angle) and the smallest head (diameter ∼2″) among all three ProPlyDs, with the largest peak flux at 3 cm while the integrated head flux is comparable. Its head-to-tail flux ratio is about 10 : 1, whereas in the other two ProPlyDs part of the tail might be confused with the head flux density.

Both ProPlyD 1 and 2 appear inclined with respect to the plane of the sky, the latter one slightly, the former one probably in a major way. This can be seen e.g. in Fig. 2 where we have indicated the projected direction to the ionizing source. The residual map of ProPlyD 1 shows clearly two excess emission sites, one corresponding to the tail, and a second one north of it. Recent Hα images support the idea of ProPlyD 1 actually being composed of two cometary-shaped objects. Thus we interpret this northern excess as the second head. A two Gaussian fit to ProPlyD 1 at 3 cm gives peak fluxes of 3.17 mJy beam^{-1} and 3.33 mJy beam^{-1}, and (6.16 $\pm$ 0.15) mJy and (6.33 $\pm$ 0.22) mJy for the two heads, while it failed at 6 cm.

The tails of all three ProPlyDs directed away from the star cluster, approximately coincident with the tails in Hα within the positional uncertainty of the radio/optical pointings (see Fig. 2; note the relative shift of 0.″5 in declination and right ascension which we have employed in these figures). The uncertainty of the radio position is ∼0.″15 while HST has a pointing uncertainty of $< 1''$.

Possible flux variability on timescales days expected from e.g. flaring pre-main sequence (PMS) stars with non-thermal radio spectra, cannot be tested with the present data.

[INTERNAL NOTE: I have erased former Fig 4 (the brightness profiles) and the few corresponding sentences in the text because it appears we have nothing important to conclude from them.]

EDITOR: PLACE TABLE 2 HERE.

3.2. ProPlyD spectral indices

The radio continuum fluxes (see Table 2) are a factor of 8 to 21 larger than those predicted by Brandner et al. (2000) assuming optically thin thermal bremsstrahlung as the radio emission mechanism (McCullough et al. 1995), which scales with the (extinction corrected) Hα flux. The neutral part of the ProPlyD envelope may attenuate Hα photons from the far side of the object depending on the viewing angle. However, McCullough et al. (1995) have estimated this effect to be less than 25% of the total Hα light for an isotropic ensemble of ProPlyDs. Furthermore, the reasonable coincidence of the ProPlyD sizes in the radio and optical band suggests that this effect is not important here. The integrated flux at 6 cm is significantly higher than that at 3 cm (except for ProPlyD 2), whereas similar flux densities were predicted. The average spectral indices of ProPlyD 1 and 3 appear negative with values between –0.2 and –0.5 ($S_\nu \propto \nu^\alpha$), indicating non-thermal emission, while the spectrum of ProPlyD 2 is in agreement with the expectation from optically thin thermal bremsstrahlung.

Because of the high resolution and sensitivity in the radio maps we were able to generate spectral index maps for all three ProPlyDs. We used only brightness densities greater than 0.8 mJy beam^{-1}, which corresponds to roughly 4 σ at 6 cm and 8 σ at 3 cm. Fig. 4 shows the resulting spectral index maps. The radio emission zone within each ProPlyD appears not to be homogenous. The spectra are generally steeper in the tail than

in the head with a tendency of positive spectral indices located towards the region facing the ionizing star cluster. Though the spectrum in the tail suffer from large uncertainties due to the low flux densities, the fact that *systematically all* three tails show non-thermal spectra, whereas the low flux density rim of the region opposite to it shows positive spectral indices, supports the idea of a *real* spectral trend.

3.3. Extinction towards the ProPlyDs

Melnick et al. (1989) have derived the reddening towards NGC 3603 from UBV photometry, and found $A_V \approx 4 - 5$ mag for the cluster core. However, as can be seen in their data, the visual extinction is not uniform across the whole starforming region, but increases significantly when moving away from the star cluster. For example, star MTT 68, close to ProPlyD 3, has $A_V \approx 6.2$, whereas star MTT 81 near ProPlyD 1 has $A_V \approx 4.7$, and star MTT 79 close to ProPlyD 2 has extinction $A_V \approx 5.2$. Here we have used $R = A_V/E_{B-V} \approx 3.2$ as determined by Melnick et al. (1989) for NGC 3603. Thus, it appears likely that the ProPlyDs suffer from stronger foreground extinction than the stars in the cluster center.

Using the ratio between radio flux density and Hα flux as given by (McCullough et al. 1995, their equation 5) and assuming that the radio flux density at 3 cm is dominated by thermal bremsstrahlung, we predict the Hα flux using our 3 cm radio continuum data. The predicted fluxes are then compared to the Hα fluxes measured by Brandner et al. (2000) and used to derive lower limits for the extinction, $A_{H\alpha}$. (For the case of (gyro)synchrotron radiation as the radio emission process, coming from an emitting region as specified in Sect. 4.4, the necessary extinction would be even higher with the exact value depending on the magnetic field.) Table 3 shows the calculated fluxes (assuming $T_e = 10^4$ K) and extinctions. Note the uncertainty in comparing different areas for which the Hα fluxes and

the radio continuum fluxes have been obtained. Brandner et al. (2000) give the Hα surface brightness of the ProPlyD heads, measured for a 0.″5 aperture radius, whereas we quote peak fluxes per beam where the beam size is 0.″95×0.″95. For $A_{\mathrm{H}\alpha} \approx 0.85 A_{\mathrm{V}}$, we find $\mathrm{A_V} \approx 6.4$ for ProPlyD 1 and $\mathrm{A_V} \approx 7.3$ for ProPlyD 2. We find significant excess extinction for both ProPlyDs, which may be intrinsic to the ProPlyDs themselves, otherwise the extinction estimate derived from the stars is underestimated. Thus, the varying extinction across the starforming region in NGC 3603 can not explain the inconsistency between predicted and observed radio flux level.

EDITOR: PLACE TABLE 3 HERE.

3.4. ProPlyD densities and mass-loss rates

Estimates for the electron/ion density inside the ProPlyD heads can be obtained from our radio data if thermal bremsstrahlung dominates the radio emission. This is likely the case for ProPlyD 2 and maybe 3, while for ProPlyD 1 the derived values should be considered as upper limit. The bremsstrahlung intensity in the radio domain for a thermal, ionized H-gas of constant density in a sphere is (Mezger and Henderson 1967)

$$S_{\mathrm{radio}} \approx 1.9 D_{\mathrm{kpc}} \theta_{\mathrm{sec}}^3 N_{e,4} N_{\mathrm{ion},4} \nu_{\mathrm{GHz}}^{-0.1} T_4^{-0.35} \mathrm{mJy},$$

where D_{kpc} is the source distanc in kpc, θ_{sec} is the apparent radius of the source in arcsec, $N_{e,4}$ and $N_{\mathrm{ion},4}$ are the electron and ion density, respectively, in 10^4 cm^{-3}, ν_{GHz} is the observing frequency in GHz and T_4 is the electron temperature of the ionized gas in 10^4 K. We use the values in Table 2 for the source size. For $T_4 = 1$ and $N_e \approx N_{\mathrm{ion}}$ we estimate the electron density by comparing the expected radio flux with the observed 3 cm ProPlyD head flux densities, and find $N_e = 9 \cdot 10^3$ cm^{-3} for ProPlyD 1, $7 \cdot 10^3$ cm^{-3} for ProPlyD 2 and

$12 \cdot 10^3$ cm^{-3} for ProPlyD 3. (The corresponding emission measures are $5.4 \cdot 10^6$ cm^{-6} pc, $3.7 \cdot 10^6$ cm^{-6} pc and $8.1 \cdot 10^6$ cm^{-6} pc for ProPlyD 1, 2 and 3, respectively.) These are in reasonable agreement with $N_e \geq 10^4$ cm^{-3} derived from [SII] line ratios by Brandner et al. (2000). For the Orion ProPlyDs densities of order $10^5 - 10^6$ cm^{-3} have been found (Henney and O'Dell 1999). Note that our derived numbers suffer from uncertainties due to the unknown projection angle of the ProPlyDs, and hence the true source diameter.

Mass loss in ProPlyDs occurs through external heating of the envelope by the far ultraviolet (FUV) radiation field from hot stars, especially from the core of NGC 3603, and subsequent evaporation. Knowing the electron density the mass-loss rate in a wind is given by $\dot{M} = 4\pi R^2 \mu m_H v_W$, with R the system radius, m_H the ion mass and v_W the evaporation velocity. Assuming a pure hydrogen gas, $\mu = 1.3$, we find $\dot{M}/v_{20} \approx (8-10) \times 10^{-5}$ M$_\odot$year^{-1} for the heads of all three ProPlyDs, where v_{20} is the wind velocity in units of 20 km s^{-1}. Brandner et al. (2000) found evaporation flow velocities of order 10-25 km s^{-1}. The so derived upper limits for the mass-loss rates are of the same order as estimated by Brandner et al. (2000), and about two orders of magnitude higher than the typical values for the Orion ProPlyDs.

A very rough estimate of the mass reservoir of the NGC 3603 ProPlyDs can then be derived by multiplying the mass loss rate with an estimated evaporation time scale of $\sim 10^5$ years (Brandner et al. 2000). This gives a ProPlyD mass of order 1-10 M$_\odot$, 10–1000 times larger than for the Orion ProPlyDs. The radius of the putative disks in these massive objects can be estimated using the evaporation model of Johnstone et al. (1997) which considers the mass reservoir in a disk-like shape. We find an approximate disk radius of 2000 AU ($\approx 0.3''$) for all three NGC 3603 ProPlyDs.

4. Discussion

4.1. Comparions with the ProPlyDs in the Orion and Lagoon Nebulae

The ProPlyDs in NGC 3603 are 20–30 times larger and much more spectacular than those in Orion, which were detected at 2 and 20 cm with the VLA (see McCullough et al. (1995) and references therein, Henney and O'Dell (1999)).

Orion contains numerous dense clumps, originally classified as UC H II regions, but now known to be ProPlyDs. Most Orion ProPlyDs have central disks, sometimes seen only in silhouette against the background light. On recent HST-images dozens of jets powered by young stars embedded in ProPlyDs have been found (Bally et al. 2000). All Orion ProPlyDs detected at radio wavelengths are non-variable thermal emitters with spectral indices between –0.1 and 0.2 (Felli et al. 1993), and located within 0.04 pc of the ionizing O-star (θ^1 Ori C). The non-thermal Orion radio sources show strong variability, and are mostly associated with visible PMS stars. Their non-thermal spectra are usually explained as due to stellar flaring activity.

G5.97–1.17 (D = 1.8 kpc) is an ultracompact H II region at $\sim$ 5000 AU projected distance from the O7 star Herschel 36 in the center of M8, the Lagoon Nebula (Stecklum et al. 1998). ESO near-infrared, HST optical and VLA radio continuum observations indicate that G5.97–1.17 is a young star surrounded by a circumstellar disk that is likely being photo-evaporated by Her 36, similar to the so-called ProPlyDs in Orion. The previous hypotheses suggested that G5.97–1.17 is a UC H II region intrinsically ionized by an embedded B0 star. However, Stecklum et al. (1998) showed that G5.97–1.17 is predominantly externally ionized, and thus the spectral type of the embedded star should be later than B5. The Hα flux over 0.″6 is consistent with the λ = 2 cm appearance. Optical and near infrared (NIR) continuum images show the central star displaced from the peak

of the bow shock by 0.″125. NIR photometry of G5.97–1.17 revealed that its central star is extremely red, which cannot be explained by extinction laws that use spherical matter distributions. This supports the idea of the circumstellar matter surrounding the central star of G5.97–1.17 being arranged as a disk. The cm-radio spectrum of G5.97–1.17 appears flat, which is interpreted as optically thin free-free emission (Wood and Churchwell 1989; Doherty et al. 1994). No OH or H_2O masers, which are often associated with UC H II regions, are known in G5.97–1.17.

In comparison, the NGC 3603 ProPlyDs appear rather peculiar and spectacular. Not only are they the largest and most massive ones found so far. Exposed to an extremely strong FUV radiation field, they also suffer the largest mass losses, though their distance to the ionizing source appears to be larger than for the Orion or Lagoon Nebula ProPlyDs. No embedded source nor disk has been found for any of the NGC 3603 ProPlyDs. At cm-wavelengths they are so far the only ones showing non-thermal behaviour.

Peculiar also is the spatial distribution of the NGC 3603 ProPlyDs. They are not only distributed apparently along one straight line (see Sect. 4.3 for further discussion), but also lie strictly north of the stellar cluster, ionized gas region and the molecular cloud. This is in clear contrast to the Orion ProPlyDs which does not appear to be located in prefered regions of the nebula (e.g. Bally et al. (2000)). Since sequential star formation proceeding from north to south seems evident in NGC 3603 (e.g. De Pree et al. (1999)), this raises the question whether the ProPlyD-like structures in this region have been formed just recently.

EDITOR: PLACE TABLE 4 HERE.

4.2. External versus internal ionization

A possible way to prove that the ProPlyDs have indeed been ionized *externally* by the star cluster is to show that the observed ProPlyD radio fluxes are consistent with the number of ionizing photons they receive from the cluster stars. For simplicity we assume a thermal radio emission mechanism here, and note that this leads to rather an upper limit for the number of ionizing photons needed to produce the observed radio flux density. In this case the brightness temperature is directly proportional to the number of ionizing photons. Because in NGC 3603 a large number of stars are extremely hot and luminous it provides an ionizing flux that is several orders of magnitude larger than in Orion or M 8 (see Table 4). The expected brightness temperatures at the projected ProPlyD distances of 1.3 pc, 2.2 pc and 2.0 pc from the ionizing source due to a Lyman flux of 10^{51}photons s^{-1} (Brandner et al. 2000) are 200 K, 70 K and 90 K at 3 cm assuming $T_4 = 1$. This is only slightly higher than our estimates derived from the *ATCA* 3 cm maps of 40 K, 30 K and 60 K for the three ProPlyDs, respectively. We can also compare the number of ionizing photons required to deliver the observed flux densities at the location of the ProPlyDs, and compare this number with the number of Lyman photons they receive from the star cluster. Noting that the ProPlyDs subtend an area of $6 \cdot 10^{-5}$, $3 \cdot 10^{-5}$ and $2 \cdot 10^{-5}$ of the total solid angle seen by the cluster stars, they receive thus $6 \cdot 10^{46}$, $3 \cdot 10^{46}$ and $2 \cdot 10^{46}$ photons s^{-1}, respectively. On the other hand, the required number of ionizing photons at the location of each ProPlyD to deliver the observed radio flux density is about $2 \cdot 10^{46}$ photons s^{-1} in all three cases. These comparisons show that the number of required Lyman photons is slightly lower than provided by the star cluster, and thus would even allow an additional dust attenuation and/or more likely longer linear distances between the ProPlyDs and the ionizing source in the external ionizing scenario. Significant ionizing power from the putative central point source inside the ProPlyDs appears therefore unlikely, which puts its spectral type to later than ~B1.

4.3. Does the proplyd-like objects host disks ?

The present radio data as well as the recently published HST/VLT-images do not provide direct evidence that the observed proplyd-like objects in NGC 3603 host any (proto-)stellar objects and disks at all. In fact, down to a limiting K_s-magnitude of 18 mag, no circumstellar disk nor central stellar object in either ProPlyD has been detected by HST+VLT observations Instead the cometary-shaped nebulae may rather be massive emission regions photo-ionized by the radiation from the star cluster. Mellema et al. (1998), e.g., presented model calculations for such clumps, called FLIERs or ANSEA (commonly located along the major axis of the ionizing source). Indeed, all three ProPlyDs apparently lie approximately along one straight line, with the outflow source Sher 25 roughly in the middle between ProPlyD 1 and 3. Though the bipolar outflow from Sher 25 appears not to point into the direction of the three extended sources, the ring-like structure around Sher 25, roughly perpendicular to the jet, has been shown to expand with a velocity of $\sim$ 30km s^{-1} (Brandner et al. 1997), and could in principle be the origin of the ProPlyD-like clumps. However, the most likely different inclination angles of the three ProPlyDs with respect to the plane of the sky renders this scenario of Sher 25. Problematic furthermore, models which are not based on disk-like mass distributions, like e.g. the FLIER model, typically give short evaporation times, inconsistent with the distance of the ProPlyDs from Sher 25 (W. Brandner, private communication) and the approximate date of the mass-loss event about 6630 years ago in Sher 25 (Brandner et al. 1997). Thus, the data appear to favour models where most of the material is concentrated in compact structures like, e.g. disks, however, any direct evidence is still missing.

4.4. The possible origin of the non-thermal emission

Our finding of non-thermal spectra from the ProPlyDs, steepest in the tails, slightly flatter in the heads, and with a tendency of positive spectral indices ($S_\nu \propto \nu^\alpha$) located towards the region facing the ionizing star cluster rather than away from it appears to rule out non-thermal radio emission from a wind–wind collision region. The non-thermal radiation must originate rather from inside the ProPlyDs, either from their putative central stars hidden behind thick material, the surrounding disks or the envelopes. Non-thermal radio spectra could be produced by a population of energetic particles emitting synchrotron, gyrosynchrotron or gyroresonance radiation in a magnetic field.

4.4.1. Stellar origin ?

Non-thermal radio emission has been observed from pre-main sequence (PMS) stars, where (gyro)synchrotron emission is explained by accelerated particles in magnetic loops close to the star surface during flaring activity. Prototypes of such PMS non-thermal sources are DoAr21 in ρ Ophiuchus (Feigelson and Montmerle 1985), V410 Tau (Cohen and Bieging 1986) or T Tauri (Skinner and Brown 1994). Similar processes are thought to occur in RS CVn stars (which have radio luminosities in the same range as PMS stars), but here the magnetic loops are believed to be more extended, as large as the binary separation. RS CVn stars are, however, believed to be in a post main sequence stage of evolution, and thus much older than the average age of the core of NGC 3603 (which lies between 2–3 Myr with a spread of up to ± 2 Myr (Melnick et al. 1989)), and is therefore unlikely to be the origin of the observed non-thermal emission in any member of this star forming region. Non-thermal stellar PMS sources have also been observed from the Orion region (e.g. Felli et al. (1993)). They all appear variable, as expected from the flaring model, with cm-radio luminosities in the range of $10^{26} - 10^{27}$ erg s^{-1}, whereas the radio luminosities of the NGC 3603 ProPlyDs

are several orders of magnitudes higher, $(4-8) \times 10^{31}$ erg s^{-1}, the expected radio luminosity of extremely bright massive stars. Also, the non-thermal processes occur relatively close to the star surface, and thus would have difficulties in explaining non-thermal radio spectra from a tail extended over several 10^{-2} pc.

The commonly observed X-ray emission from young stellar objects (YSOs) appears to be correlated with the cm-radio luminosity (e.g. André et al. (2000)). Following this relation, the expected X-ray luminosity for a possible embedded proto-/PMS star in the NGC 3603 ProPlyDs should be $> 10^{33}$ erg s^{-1}. No point source clearly associated with the ProPlyDs was detected during a recent 50 ksec *Chandra* ACIS-I observation of NGC 3603 above the sensitivity limit of $\sim 10^{-15}$ erg cm^{-2} s^{-1} in the range 0.1-10 keV [6], implying an unrealistically high column density of absorbing material associated with the ProPlyDs themselves of at least 10^{25} cm^{-2} (assuming interstellar abundances) if the observed cm-radiation is due to solar-type activity from an embedded YSO. Note that a X-ray luminosity of $L_X \sim 5 \cdot 10^{30}$ erg s^{-1} corresponds to the above mentioned sensitivity at 6 kpc distance assuming a column density of $N_H \sim 10^{22}$cm^{-2}, appropriate for NGC 3603. Thus, the hidden YSO scenario appears difficult.

The observed radio luminosity might be reached by a massive star/binary brighter than any one detected so far in NGC 3603. As discussed above, this source cannot be of spectral

---

[6]The point source close to ProPlyD 3 found on HST-images is actually lying in front of the envelope (Brandner et al. 2000), and is thus most likely not physically associated with it. Recent *Chandra* observations (Moffat et al., in preparation) have revealed an X-ray point source of luminosity $\sim$?? erg s^{-1}, located between the radio and optical source (see Fig. 1 and 2). Given the fact that no X-ray point sources were found close to ProPlyDs 1 and 2, we consider the *Chandra* source near ProPlyD 3 as a likely counterpart of the optical point source, and thus not physically related to the ProPlyD.

type earlier than B1. Radio luminosities of B0-B8 supergiants lie at $\leq 10^{29}$ erg s^{-1} (Scuderi et al. 1998), insufficient to explain our radio data. In addition, wind velocities from massive stars are typically two orders of magnitude larger than the values implied by the HST-data (Brandner et al. 2000). Radio flare stars may reach the observed radio luminosities during flaring activity, however, again the age of these stars makes this scenario rather unlikely.

4.4.2. Non-stellar origin

Disk or envelope, whatever the ultimate source might be, the clearly negative spectral indices suggest optically thin non-thermal processes as the radiation mechanism for most regions in ProPlyD 1 and 3. One could, e.g., argue that the shock created by the evaporation flow in ProPlyD models could accelerate charged particles within the objects. Other possibilities may be inflow-outflow activity causing shocks during the early stage of star formation, compression and reconnection of magnetic fields in the collapsing envelope, or magnetic reconnection in star–disk interactions in YSOs leading to production of energetic particles. Magnetic fields are known to exist in Molecular Clouds (Crutcher 1999), and therefore it appears plausible that gas clumps still contain "fossil" fields. In a magnetized plasma, acceleration due to particle collisions and subsequent bremsstrahlung can often be negligible in comparison with acceleration due to gyration around the field lines. In place of free-free emission, one then has (gyro)synchrotron emission from (mildly) relativistic particles. The negative radio spectral indices in ProPlyD 1 and 3 are conveniently explained by non-thermal particle spectra. Because the thermal bremsstrahlung is proportional to $N_e^2 T_e^{-1/2}$ and the gyrosynchrotron emission is proportional to $N_e T_e^{\xi} B^{\beta}$ (ξ,$\beta > 0$), the former dominates if the density is high enough, or if the temperature or field strength is low enough. Indeed the electron densities found in the NGC 3603 ProPlyDs are several orders of magnitude smaller than in the Orion ProPlyDs (see Table 4). The different energy

dependencies of the two kinds of emission may lead to one dominating at low frequencies and the other at high frequencies. Note, however, that a non-thermal spectrum may mimic thermal free-free emission. E.g. free-free absorbed gyrosynchrotron radiation produces flat spectra in the frequency range $30 \leq (\nu_{\rm ff}/\nu_B) \leq 70$ (e.g. Ramaty and Petrosian (1972)) where $\nu_B \approx 2.8 \cdot 10^{-3} B_G$ GHz is the gyrofrequency, B_G is the magnetic field strength in Gauss, and $\nu_{\rm ff} \approx 0.7 (EM)^{1/2} T_e^{-0.75}$ GHz is the frequency where the optical depth for free-free absorption is unity, with EM the emission measure in units cm^{-6} pc.

A lower limit for a possible magnetic field can be given by using the Razin-Tsytovich effect. In order to avoid a Razin-suppression of the radio spectrum above 6 cm the magnetic field cannot be smaller than $\sim 10^{-5}$ G for an electron density of 10^4 cm^{-3} in the emission region. On the other hand, to avoid gyroresonance absorption above 20 cm the field strength cannot be higher than 10^3 G. The equipartition magnetic field, the minimum possible value in flare loops, for a $T_e = 10^4$ K particle distribution with density 10^4 cm^{-3}, is $\sim 10^{-3}$ G. For gyrosynchrotron radiation the emission is concentrated at harmonic numbers $s = \nu/\nu_B = 10 - 100$. This additionally constrains the possible range of magnetic fields to $B \approx 20 - 200$ G for the case of gyrosynchrotron radiation while for synchrotron emission the likely field strength ranges from $\sim 10^{-3}$ G (the equipartition field) to about 10^3 G (derived by requiring the 6 cm flux density to be synchrotron photons of frequency $\nu_{\rm syn} \simeq 4 E_{\rm MeV}^2 B_G$ MHz for an electron energy $E_{\rm MeV}$ in units MeV, which cannot be smaller than $E_{\rm MeV} = 1$). Note that synchrotron photons of energy 4.8 GHz in a 10^{-3} G field must have been produced by ~ 500 MeV electrons.

Dulk (1985) gives an approximate formula for the gyrosynchrotron radiation from a mildly relativistic plasma for the range s = 10–100 of harmonic numbers and viewing angle 20° - 80°. Our data require an underlying particle distribution which follows approximately a E^{-2} power law. For an electron distribution with power law index -2 above 10 keV the

flux density due to optically thin non-thermal gyrosynchrotron emission is then

$$S_{\nu,\mathrm{gyro}} \approx 4.9 \times 10^{16} N_{e,4} B_G^{1.59} l_{\mathrm{pc}}^3 D_{\mathrm{kpc}}^{-2} \nu_{GHz}^{-0.59} \ \mathrm{mJy}$$

assuming a uniform randomly distributed magnetic field, constant electron density, and l_{pc} is the source diameter in pc. Using $l_{\mathrm{pc}} = 0.03$, $N_{e,4} = 1$ and $B_G = 20 - 200$ we find flux densities $10^{12} - 10^{13}$ times higher than observed. Similar results are obtained when using different density and field distributions, e.g. a dipole field.

In the case of synchrotron radiation in a uniform field the flux density of a homogenous sphere with diameter l and low energy cutoff $E_{\mathrm{min,MeV}}$ in units MeV of a E^{-2} particle distribution is given by (see e.g. Dulk 1985)

$$S_{\nu,\mathrm{syn}} \approx 3.4 \times 10^{18} N_{e,4} B_G^{1.5} E_{\mathrm{min,MeV}} l_{\mathrm{pc}}^3 D_{\mathrm{kpc}}^{-2} \nu_{GHz}^{-0.5} \ \mathrm{mJy}$$

Since N_e cannot be significantly smaller in order not to contradict the optical data if the radio and optical emission originates from the same site, we are led to conclude that the size of the actual magnetized emitting volume V_{emi} is reduced by at least a factor $f \approx 10^{-12}$ if the radio emission is due to gyrosynchrotron radiation, and by a factor $f \approx 10^{-15} - 10^{-6}$ for the case of synchrotron radiation. With $f = V_{\mathrm{emi}}/V_{\mathrm{tot}}$ this gives $V_{\mathrm{emi}} \approx 3$ AU^3 for gyrosynchrotron emission, and brightness temperatures of the emitting region then reach values $10^8 - 10^9$ K, indicative of non-coherent, non-thermal processes. Though it is evident that the emitting region must be much smaller than the extent of the ProPlyD, the present data do allow a wide range of values for this proportionality factor f. The uncertainty of the f-value is predominantly caused by the wide range of possible field strengths, and to a lower degree by the uncertain value of the electron density (note that according to Brandner et al. (2000) $N_{e,4} = 1$ is rather a lower limit, and thus the given f-value an upper limit) and a $\sim 10\%$ uncertainty of the source distance.

We note that our suggestion of an emission region significantly smaller than the appearance of the ProPlyD on the sky is in remarkable agreement with the recent findings

of Schulz et al. (2000), who discovered X-ray emission from some ProPlyDs in Orion, and thereby could constrain the actual size of the emitting region to order 1-10 AU on the basis of variability arguments.

Typical magnetic field strengths in molecular clouds reach values of $B_{\rm MC} \approx 1 - 10^3 \mu$G (Crutcher 1999). Furthermore, Crutcher (1999) found an average scaling of their magnetic fields with density ρ of $B \propto \rho^{0.5}$. Applying mass conservation this proportionality transforms into $B \propto R^{-1.5}$ where R is the system size. Thus, if the emitting region has been formed from material of the molecular cloud in the course of a local collapse, which appears likely, then the magnetic field $B_{\rm emi}$ of the emission site is expected to reach values of $B_{\rm emi} \approx f^{-0.5} B_{\rm MC} \approx 1 - 10^3$ G for $f \simeq 10^{-12}$ or $B_{\rm emi} \approx 10^{-3} - 1$ G for $f \simeq 10^{-6}$. This is in reasonable agreement with our derived field strength requirements.

5. Summary and Conclusions

The three massive (~ 1 $M_\odot$) ProPlyDs in NGC 3603, which have been recently discovered by Brandner et al. (2000), have been clearly detected and resolved with the *ATCA* at 3 and 6 cm, with one of them probably actually composed of two cometary-shaped objects. Their flux densities are about 10–20 times higher than expected from the Hα measurements, and a non-thermal average spectrum can be associated with at least two of the YSOs. This is the first time that radio emission from a ProPlyD turns out to be of non-thermal origin. Our spectral index maps show that the emission region is rather inhomogenous, with negative spectral indices in the tail and part of the head whereas positive spectral indices, indicating thermal free-free emission, tend to be detected from a small region facing the star cluster.

We derive upper limits for the mass-loss rates and electron densities, which turn out to

be in reasonable agreement with the estimates from recent HST-images.

We show that (gyro)synchrotron emission from a magnetized, (mildly) relativistic, non-thermal particle population might be able to explain the non-thermal spectral regions in the ProPlyDs 1 and 3, provided the actual emitting volume is significantly smaller (no more than $f \approx 10^{-6}$) than the extent of the ProPlyD envelopes at radio wavelengths, if the optical and radio photons originate from the same region. Energetic particles necessary for (gyro)synchrotron radiation might be produced through shocks or by magnetic reconnection.

The extremely high radio luminosities of $\sim 10^{31-32}$ erg s^{-1} of the ProPlyDs together with their low wind speed and missing X-ray emission make a stellar origin of the radio emission unlikely. In addition, the observed radio fluxes are consistent with a predominantly *external* source of ionization. Thus magnetic fields, which have been neglected in ProPlyD models so far, are possibly associated with the ProPlyD envelopes or disks, and appear to be crucial in understanding the physical processes in these ProPlyD-like objects. The lack of any hint for a central stellar object or disk questions their identification as ProPlyDs though.

Melnick et al. (1989) has shown that an inhomogenous dust distribution in NGC 3603 causes increasing extinction with distance from the star cluster. In particular, the extinction at the location of the ProPlyDs is estimated to lie between $A_V \approx 5 - 6$ mag. We show that these values are, however, not sufficient to explain the unexpected high radio- to Hα-luminosity ratio.

The discoverage of the so-far undetected disks which are thought to be part of all ProPlyDs may give important hints about the origin of the extremely high and non-thermal radio fluxes and the nature of the cometary-shaped clumps.

We are grateful to Wolfgang Brandner for providing the HST image of NGC 3603

to overlay on our radio images, for interesting discussions and carefully reading the manuscript. We like to thank Jessica Chapman, Jim Caswell, Simon Johnston, Tylor Bourke and Sergey Marchenko for reading the manuscript and many constructive comments which improved our paper significantly. AM acknowledges a postdoctoral bursary from the Quebec Government. AFJM thanks NSERC (Canada) and FCAR (Quebec) for financial support. ...

REFERENCES

André P., 1996, in: "Radio Emission from the Stars and the Sun", eds. A.R. Taylor, J.M. Paredes, Vol. 93, 273, San Francisco, ASP

Bally, J., O'Dell, C.R. and McCaughrean, M.J., AJ, 119,2919

Brandner, W., et al. 1997, ApJ, 489, L153

Brandner, W., et al. 2000, AJ, 119, 292

Cohen, M. and Bieging, J.H., 1986, AJ, 92, 1396

Crowther, P.A. and Dessart, L., 1998, MNRAS, 296, 622

Crutcher, D., 1999, ApJ, 520, 706

De Koter, A., Heap, S.R. and Hubeny, I., 1997, ApJ, 477, 792

De Pree, C.G. et al. 1999, AJ, 117, 2902

Doherty, R.M. et al. 1994, MNRAS, 266, 497

Dulk, G.A. 1985, ARA&A, 23, 169

Feigelson, E.D. and Montmerle, T., 1985, ApJ, 289, L19

Feigelson, E.D. and Montmerle, T., 1999, ARA&A, 37, 363

Felli, M., Taylor, G.B., Catarzi, M., Churchwell, E. and Kurtz, S., 1993, A&AS, 101, 127

Henney, W.J. and O'Dell, C.R., 1999, AJ, 118, 2350

Johnstone, D., Hollenbach, D., Störzer, H., Bally, J., Devine, D. and Southerland, R., 1997, BAAS, 189, No. 49, 12.

McCullough, P.R. et al. 1995, ApJ, 438, 394

Mellema, G. et al., 1998, A&A, 331, 335

Melnick, J., Tapia, M. and Terlevich, R., 1989, A&A, 213, 89

Mezger, P.G. and Henderson, A.P., 1967, ApJ, 147, 471

Moffat, A.F.J., Drissen, L., and Shara, M., 1994, ApJ, 436, 183

Ramaty, R. and Petrosian, V., 1972, ApJ, 178, 241

O'Dell, C.R., Wen, Z. & Hu, X., 1993, ApJ, 410, 6960

Schulz, N.S. et al., 2000, ApJ, in press

Scuderi et al., 1998, A&A, 332, 251

Skinner, S.L. and Brown, A., 1994, AJ, 107, 1461

Stapelfeldt, K., Sahai, R., Werner, M., & Trauger, J., 1997, in ASP Conf. Ser. 199, Planets Beyond the Solar System and the Next Generation of Space Missions, ed. D. Soderblom (San Francisco:ASP), 131

Stecklum, B., et al. 1998, AJ, 115, 767

Wood, D.O.S. and Churchwell, E., 1989, ApJS, 69, 831

Wright, A.E. and Barlow, M.J. 1975, MNRAS, 170, 41

This manuscript was prepared with the AAS LaTeX macros v5.0.

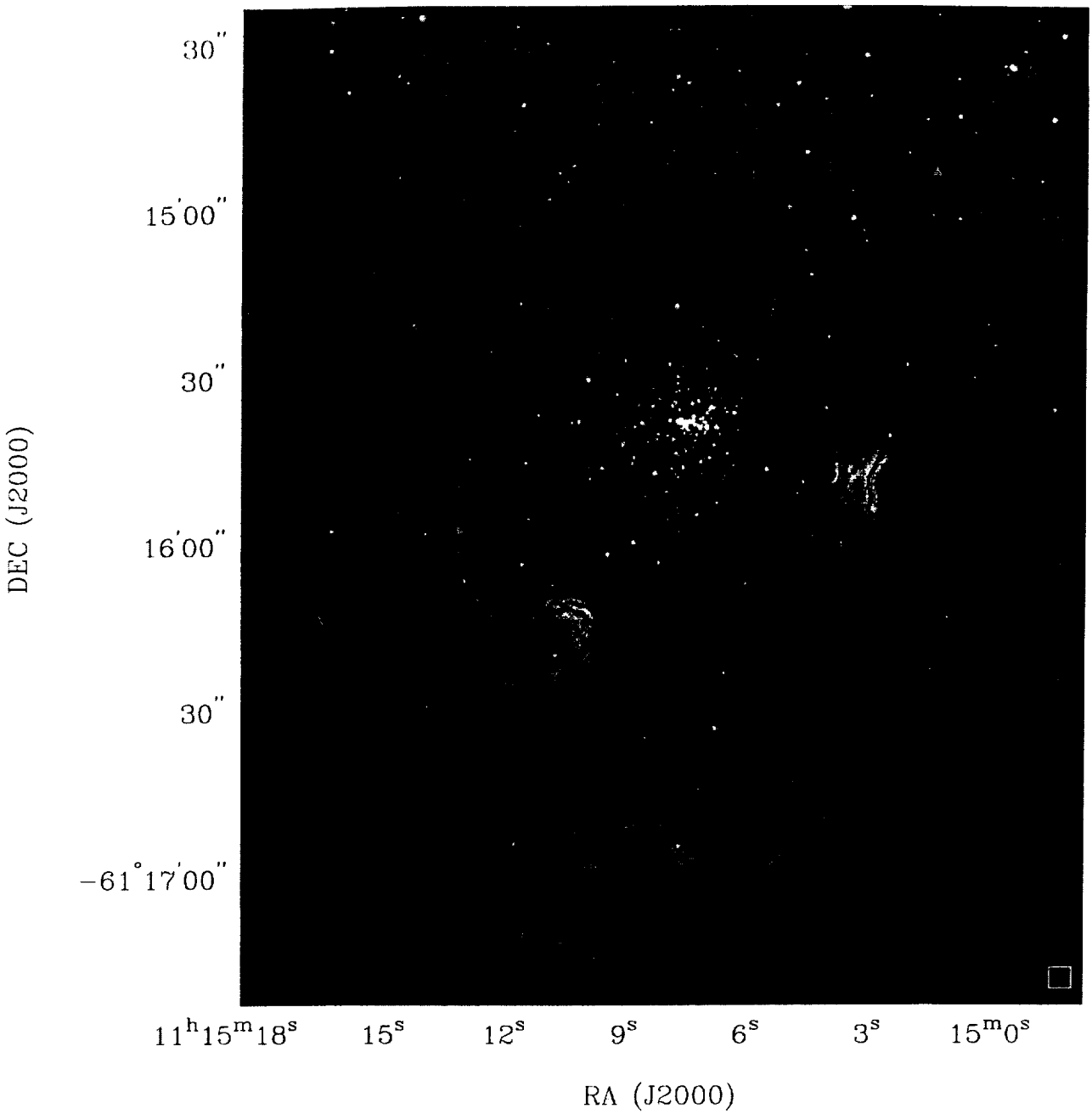

Fig. 1.— 3-cm continuum map of NGC 3603 overlaid onto the Hα and broad band HST-image from Brandner et al. (2000). Note that in this radio map the small scale structure is emphasized due to our chosen *uv*-cutoff in the data analysis. The brightest, extended continuum regions correspond to the heads of the giant gaseous pillars, showing evidence for the interaction of ionizing radiation with cold molecular hydrogen clouds. The three point-like sources, indicated with arrows, are the ProPlyDs; their tadpole shape is shown in Fig. 2. The contour levels at 3 cm are 0.85, 1.19, 1.7, 2.55, 3.4, 8.5, 17 and 34 mJy beam^{-1}.

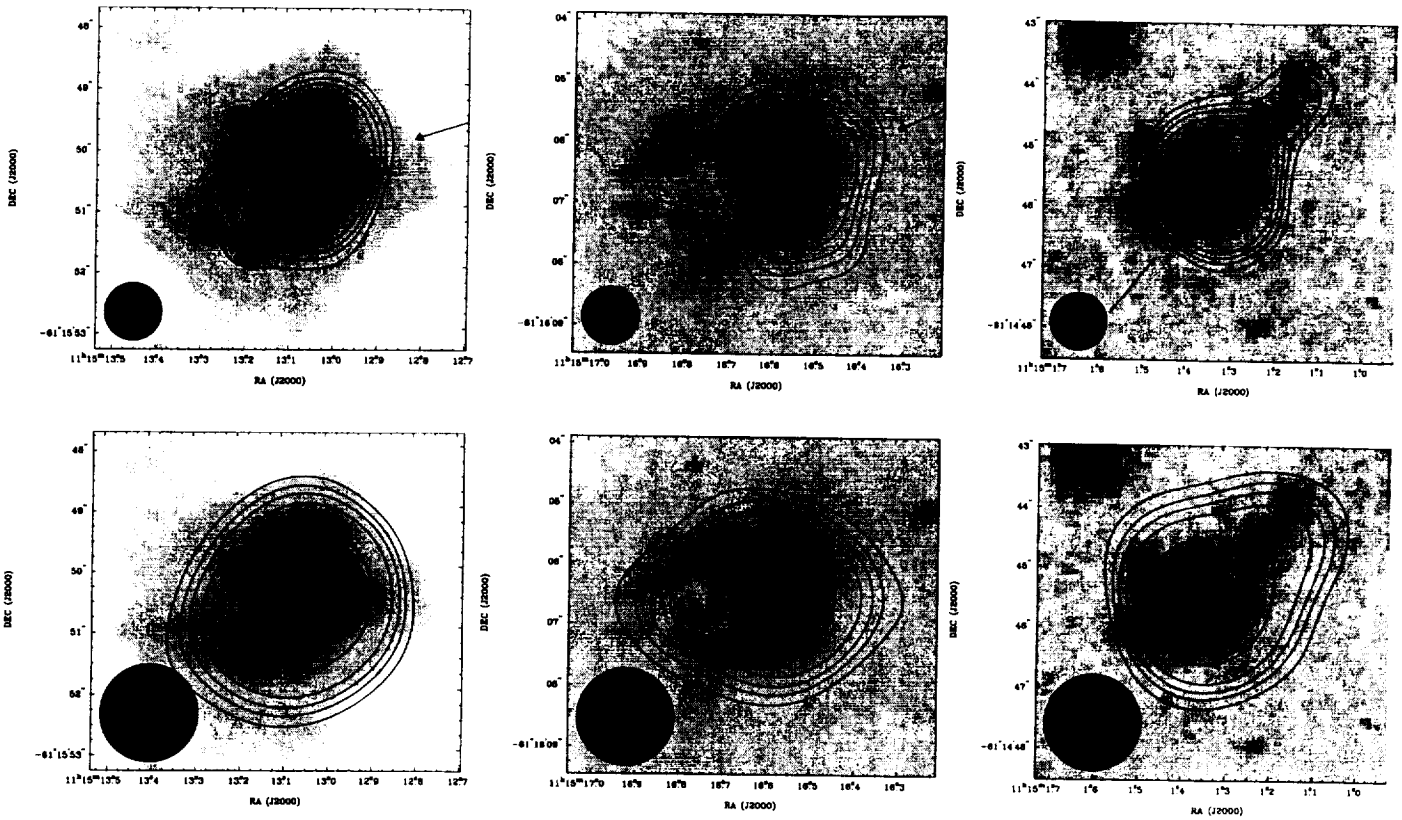

Fig. 2.— *ATCA* 3 cm (upper row) and 6-cm (lower row) radio continuum contour maps of the three ProPlyDs, numbers 1–3 from left to right, overlaid onto the Hα image from Brandner et al. (2000) for ProPlyD 1 and 2, and onto the HST broad band image for ProPlyD 3. The contour levels for the 3 cm map are 0.3, 0.5, 0.7, 1.0, 2.0, 5.0, 10 and 20 mJy beam^{-1}, and for the 6 cm map are 0.6, 1.0, 1.4, 2.0, 4.0, 10, 20 and 40 mJy beam^{-1}. The beam is shown in the bottom left corner. The Hα images have been shifted 0.″5 to the North and 0.″5 to the East in better alignment with the radio images. The arrows indicate the direction of the stellar cluster projected onto the sky. The cross near ProPlyD 3 indicates the position of the *Chandra* X-ray source.

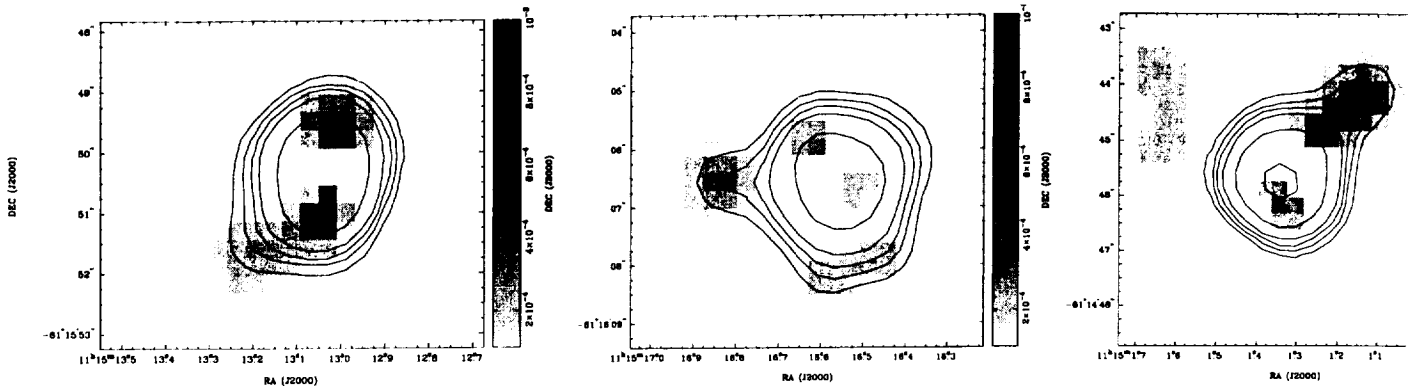

Fig. 3.— *ATCA* 3 cm residual image of the three ProPlyDs, numbers 1–3 from left to right, overlaid onto their flux density contour maps. The contour levels correspond to 0.3, 0.5, 0.7, 1.0, 2.0, 5.0, 10.0, ... mJy beam^{-1}. ProPlyD 1 appear to possess two heads.

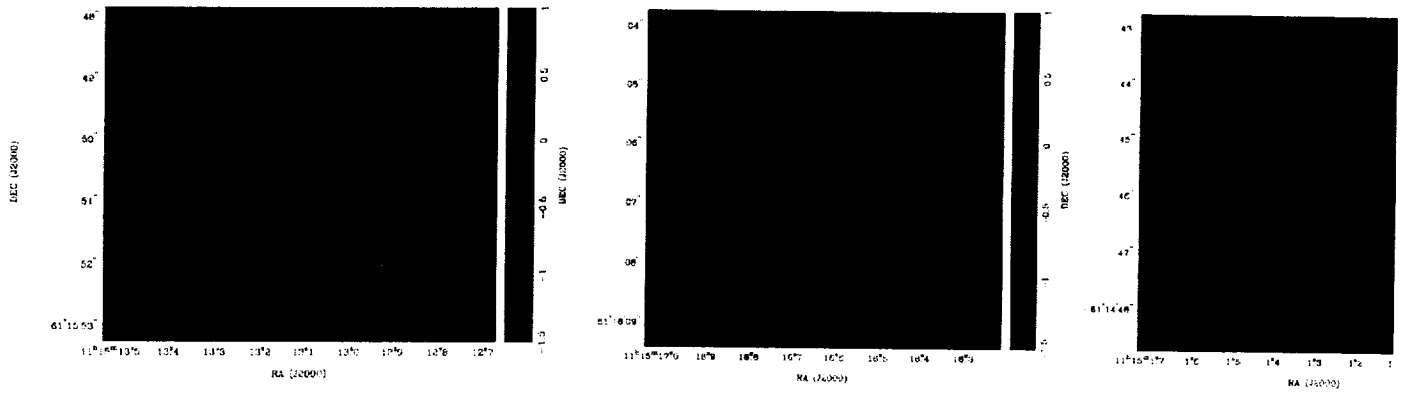

Fig. 4.— Radio spectral index map (α; colour-coded) with the corresponding uncertainty level ($\Delta\alpha$; contours) of ProPlyDs 1, 2 and 3 (from left to right). The contour levels are $\Delta\alpha$ = 0.1, 0.2, 0.3, 0.4, 0.5,.... The clip 3 and 6 cm flux value for the determination of these maps is 0.8 mJy beam^{-1}. Note the large spectral index uncertainties at the rim of the ProPlyDs due to the low flux density there.

Table 1: Observing parameters

Date	February 9/10	April 8/9	June 19
Configurations	6A	6D	6B
time on source	561 min.	514 min.	480 min.
pointing position[1]	$11^h15^m07^s$		
RA, DEC (J2000)	-61° 16′ 00″		
total bandwidth[1]	128 MHz		
No of channels[1]	32		
frequencies[1]	8640 MHz, 4800 MHz		
beam size[2]	0.″95×0.″95 (3 cm)		
	1.″61 × 1.″61 (6 cm)		
r.m.s.[2][mJy beam^{-1}]	∼0.08 (3 cm)		
	∼0.41 (6 cm)		
flux calibrator	1934–63		
phase calibrator	1059–63		

[1]the same for all three observation runs.

[2]average, for whole combined map.

Table 2: Position, fluxes and spectral indices of the ProPlyDs.

Name	ProPlyD 1		ProPlyD 2		ProPl
λ	3 cm	6 cm	3 cm	6 cm	3 cm
Radio position[1] RA,DEC (J2000)	11:15:13.042, -61:15:50.38	11:15:13.058, -61:15:50.53	11:15:16.557, -61:16:06.57	11:15:16.579, -61:16:06.62	11:15:01.336, -61:14:45.69
Axis (FWHM)[2](arcsec)	1.22	1.19	1.46	1.30	0.99
Peak flux (mJy beam^{-1})	4.77 ± 0.10[3]	10.41 ± 0.20	3.61 ± 0.10	6.78 ± 0.20	5.90 ± 0.10
Head's radio integrated flux (mJy)	12.69 ± 0.16[3]	16.08 ± 0.36	12.10 ± 0.45	11.17 ± 0.32	12.31 ± 0.18
Tail's radio integrated flux (mJy)	0.67 ± 0.10,	0.49 ± 0.20,	0.38 ± 0.10	0.67 ± 0.20	1.10 ± 0.10
Head's radio Spectral index[4]	-0.44 ± 0.05		0.12 ± 0.06		$-0.19 \pm$
Tail's radio Spectral index[4]	-0.57 ± 1.46		-2.3 ± 1.57		$-1.11 \pm$
Radio spectral index of whole ProPlyD[4]	-0.45 ± 0.07		0.05 ± 0.09		$-0.23 \pm$
$I_{H\alpha}$[5](cm^{-2}s^{-1})	0.56	0.56	0.20	0.20	—
Predicted radio flux[6](mJy)	1.56 ± 0.39	1.65 ± 0.41	0.56 ± 0.14	0.59 ± 0.15	—

Note. — The position of ProPlyD 3 given by Brandner et al. (2000; their Table 1) contains a typographical error.

[1]These positions correspond to the radio locations of the ProPlyD heads.

[2]The axes were derived after fitting a circular Gaussian to the ProPlyD head and subsequent deconvolution with the circular beam in each map. 1″corresponds to 6000 AU at the assumed distance of NGC 3603.

[3]Given here are the flux values after a one Gaussian fit, though ProPlyD 1 may possess two heads (see Fig. 3 and text).

Table 3: Estimated extinction

Proplyd		1	2	3
3 cm peak flux	[mJy beam^{-1}]	4.8	3.6	5.9
predicted Hα peak flux	[cm^{-2} s^{-1}]	2.1	1.6	2.6
derived $A_{H\alpha}$	[mag]	5.4	6.2	—

Table 4: Comparison with other known ProPlyDs.

		Orion Nebula	Lagoon Nebula	
		M 42	M 8, NGC 6523	NGC 3603
distance	[kpc]	0.45	1.8	6.1
central star(s)		Θ^1 Ori C	Herschel 36	cluster
star type(s)		O7	O7.5V	WR, O, etc.
L_{bol}	[$L_\odot$]	$\sim 10^5$	$\sim 10^5$	2×10^7
Lyman flux	[photons s^{-1}]	$\sim 8 \cdot 10^{48}$	2×10^{48}	10^{51}
extinction	[mag]	4–6	~ 5	4–6
masers		??	none known	OH, H_2O, CH_3OH
number of ProPlyDs		> 150	1 = G5.97–1.7	3
head size	[AU]	45–355	1080	7200–10800
distance to star	[pc]	0.01–0.15	0.024	1.3, 2.2, 2.0
radio flux	[mJy]	0.3–1.4	17	10–12
brightness temp.	[K]	??	~ 1500	30–90
emission measure	[pc cm^{-6}]	$8 \cdot 10^6$	$(0.3 - 2) \cdot 10^8$	$(0.9 - 2.5) \cdot 10^6$
electron density	[cm^{-3}]	$10^5 - 10^6$	$(4 - 20) \cdot 10^4$	$\sim 10^4$
mass loss rate	[$M_\odot\, yr^{-1}$]	$-1.2 \cdot 10^{-7}$	$-7 \cdot 10^{-7}$	10^{-5}
bow shock distance	[AU]	~ 100	540	44400,17400,??
velocity	[$km\, s^{-1}$]	$\sim 10 - 15$	~ 10	10–25
evap. time scale	[years]	$\sim 10^4$	$\sim 10^5$	$\sim 10^5$
ProPlyD mass	[$M_\odot$]	0.01–0.1	~ 0.1	~ 1
disk radius	[AU]	27–175	160	3400
disk mass	[$M_\odot$]	$\sim (0.5 - 20) \cdot 10^{-3}$	$\sim 6 \cdot 10^{-2}$	not known

References. — Stecklum et al. 1998, Brandner et al. 2000, Henney & O'Dell 1999, McCullough et al. 1995